

Donor-acceptor properties, catalytic activity, and negative charge exoemission from the alumina surface modified with lithium cations

A. V. Fionov,* M. V. Burova, E. A. Tveritinova, and I. V. Krylova

Department of Chemistry, M. V. Lomonosov Moscow State University,
1 Leninskie Gory, 119992 Moscow, Russian Federation.
Fax: +7 (495) 939 4575. E-mail: fionov@kge.msu.ru

Donor-acceptor properties of alumina modified with lithium cations were studied by ESR of paramagnetic complexes of adsorbed anthraquinone. The results were compared with the data on negative ion emission (exoemission) accompanying the decomposition of isopropyl alcohol in the adsorption layer. The data on the activity measured by the pulse microcatalytic technique in isopropyl alcohol decomposition are discussed. Small additives of lithium were found to promote catalytic activity of the samples. The role of acid and basic sites in isopropyl alcohol decomposition was discussed.

Key words: alumina, modification with lithium, electron-acceptor properties, electron-donor properties, ESR spectroscopy, anthraquinone, exoemission, isopropyl alcohol, heterogeneous catalysis.

Alkaline metals often exist as admixtures in Al_2O_3 -based catalysts and exert a substantial effect on the acid-base properties of the surface and, hence, on the selectivity of catalytic processes. Alumina modified with lithium cations is being studied as both a catalyst by itself^{1,2} and a support for the nickel- and manganese-supported catalysts.^{3,4} Modification is usually carried out by the impregnation method, and either hydroxide^{2,5} or a thermally unstable salt (nitrate³ or acetate⁶) is applied as a lithium compound. In the present work, the ESR and exoemission (EE) methods are used to study the acid-base properties of the $\text{Li}^+/\text{Al}_2\text{O}_3$ catalyst surface. ESR spectroscopy of paramagnetic complexes of adsorbed anthraquinone provides detailed information on the structure and concentration of electron-acceptor sites.⁷ The method of low-temperature (-269 – 420 °C) EE of negative charges gives data on the content of electron-donor sites.⁸

In the present work, we studied how a modifying lithium additive can influence the activity of the $\text{Li}^+/\text{Al}_2\text{O}_3$ catalysts in the decomposition of isopropyl alcohol and change their donor-acceptor properties.

Experimental

Catalysts were prepared by the impregnation of $\gamma\text{-Al}_2\text{O}_3$ with an aqueous solution of lithium nitrate followed by drying and calcination in air at 450 °C for 4 h and then at 600 °C for 4 h. The catalysts with a content of 0.4 – 4 mmol of Li^+ (g of Al_2O_3)⁻¹ were obtained in this way (Table 1). The surface coverage was estimated under the assumption that each Li^+ ion occupies the ion area equal to $(2r)^2$, where $r = 0.068$ nm (see Ref. 9). Then the monolayer corresponds to a coverage of $5.41 \cdot 10^{19}$ Li^+ m^{-2} or 89.8 mmol m^{-2} .

Table 1. Specific surface of the alumina samples modified with lithium cations*

Sample	Content of Li^+ /mmol (g of Al_2O_3) ⁻¹	Li : Al ratio	S_{sp} /m ² g ⁻¹	α^{**}
1	0.4	1 : 49	180	0.024
2	0.8	1 : 24.5	180	0.05
3	1.6	1 : 12	180	0.1
4	2.4	1 : 8	170	0.16
5	4.0	1 : 5	140	0.31

* The specific surface of the starting $\gamma\text{-Al}_2\text{O}_3$ sample is 185 m² g⁻¹.

** Effective coverage.

The phase composition was determined by X-ray diffraction analysis on a DRON-3M diffractometer using Cu-K α radiation.

The specific surface was measured on a GK-1 gasometer using the chromatographic method. At first, low-temperature adsorption (-196 °C) of nitrogen was carried out (using an N_2 -He mixture containing 6 mol.% N_2), then nitrogen was desorbed at room temperature, and the surface area was determined from the area of the desorption peak.

Prior to anthraquinone adsorption, the samples were subjected to thermovacuum treatment at 470 °C in air for 2 h and *in vacuo* (10^{-5} Torr) for 2 h. Anthraquinone was adsorbed using a known procedure.¹⁰ Anthraquinone (3–5 mg) was placed in an ampule sealed as a side branch to the ampule with the sample (30–40 mg). After the thermovacuum treatment, the sample was transferred to the side ampule containing anthraquinone, and the ampule was sealed off. Thus prepared ampule was kept at 120 °C for 10 h and then stored at 200 – 220 °C for a long time (to 100 h).

ESR spectra were recorded on an RE-1306 radiospectrometer at a frequency of 9.3 GHz. The concentration of paramagnetic

centers in a sample was determined by a comparison of the double integral of the spectrum through an intermediate standard (Cr^{3+} in corundum) with the absolute reference (sugar coal). The g -factors of the spectra were determined relatively to the standard, *viz.*, diphenylpicrylhydrazyl, for which $g = 2.0036$. The contribution of the eleven-component spectrum to the superposition was estimated by a comparison with model spectra obtained by the addition of the individual eleven- and six-component ESR spectra according to a known procedure.¹¹ The contribution of a single line to the superposition with the six-component spectrum was analyzed similarly.

Exoemission was detected in the pulse mode with the Geiger gas-flow counter on the Protoka industrial setup reconstructed for measuring photo- and thermostimulated EE intensities.¹² When a positive potential was fed to the detector, the emission of negative charges localized on electron-donor sites was detected. A catalyst sample (40 mg) was placed into a measuring chamber of the counter, and the background level was measured after the quenching gas (methane) was passed through the chamber. As a rule, this background exceeded the natural background of the instrument due to postemission (PE) caused by the pre-history of the sample. When the PE decayed to the level of the instrument background, thermostimulated emission (TSE) due to the thermodesorption of adsorbed particles, such as H_2O^- , O_2^- , and CO_2^- was detected during the linear heating of the sample to 360 °C. The TSE represents one or several maxima of the emission current reflecting the energy spectrum of charge localization levels on the surface. No TSE appeared upon the repeated heating of the sample.

To study the EE accompanying catalysis in the adsorption layer,¹³ a weighed sample (100 mg) of the catalyst was placed in a weighing bottle, wetted with isopropyl alcohol (100 μL), and kept for 1 day. Then the air-dry catalyst was placed in the working chamber of the counter, and the PE and TSE were detected. The PE and TSE were caused by the presence of charged particles of isopropyl alcohol and (on heating) its decomposition products, *viz.*, H_2O^- and other negatively charged particles.

Catalytic experiments were carried out in a micropulse reactor products were analyzed on a Chrom 5 chromatograph. A catalyst sample was 50 mg, and the volume of the introduced sample of isopropyl alcohol was 4 μL . Samples were activated *in situ* by heating in the reactor at 350 °C for 2 h in a nitrogen flow. The catalytic activity was measured in the temperature range from 350 to 210 °C, decreasing the temperature at an interval of 10–30 °C.

The effective apparent rate constant of catalytic decomposition of isopropyl alcohol was taken as a measure of catalytic activity¹³

$$k_{\text{eff}} = F_0 / (273 R M m) \cdot \ln[1/(1 - y)],$$

where F_0 is the rate of the carrier gas reduced to 273 K; M is the amount of introduced alcohol, m is the catalyst weight, and y is the conversion of alcohol.

Results and Discussion

Physical characteristics of samples. The specific surface of the starting $\gamma\text{-Al}_2\text{O}_3$ sample is 185 $\text{m}^2 \text{g}^{-1}$. It does not virtually change at a small lithium content and de-

creases to 140 $\text{m}^2 \text{g}^{-1}$ with an increase in the Li concentration to 2.6 mmol g^{-1} (see Table 1). The results obtained agree with published data¹⁴ according to which small additives ($<0.4 \text{ mmol g}^{-1}$) of lithium slightly change the specific surface, volume, and diameter of $\gamma\text{-Al}_2\text{O}_3$ pores. Only $\gamma\text{-Al}_2\text{O}_3$ was found in samples 1–4 by the X-ray diffraction method, while sample 5 additionally contains aluminate LiAl_5O_8 having, as $\gamma\text{-Al}_2\text{O}_3$, the spinel structure. The effective coverage (α) of the $\gamma\text{-Al}_2\text{O}_3$ surface with lithium is 0.02–0.3 monolayer capacity (see Table 1).

ESR spectra of adsorbed anthraquinone. The formation of several paramagnetic complexes was detected by ESR spectroscopy during anthraquinone adsorption on the surface of the samples under study (Fig. 1). The surface of $\gamma\text{-Al}_2\text{O}_3$ and the samples containing 0.4 and 0.8 mmole of Li^+ ($\text{g of Al}_2\text{O}_3$)⁻¹ exhibit the eleven-component ESR spectrum ($g = 2.0036$, $a = 7.4 \pm 0.2 \text{ G}$) with the intensity ratio 1 : 2 : 3 : 4 : 5 : 6 : 5 : 4 : 3 : 2 : 1. Such a hyperfine structure (HFS) corresponds to the interaction between an unpaired electron with two equivalent ^{27}Al nuclei, *i.e.*, with two coordinatively unsaturated Al^{3+} ions, which are Lewis acid sites (LAS). For a greater lithium content (samples 3–5), the contribution of the six-component ESR spectrum appears ($g = 2.0036$, $a = 9.0 \pm 0.2 \text{ G}$), whose HTS corresponds to the interaction of an unpaired electron with one ^{27}Al nucleus, *i.e.*,

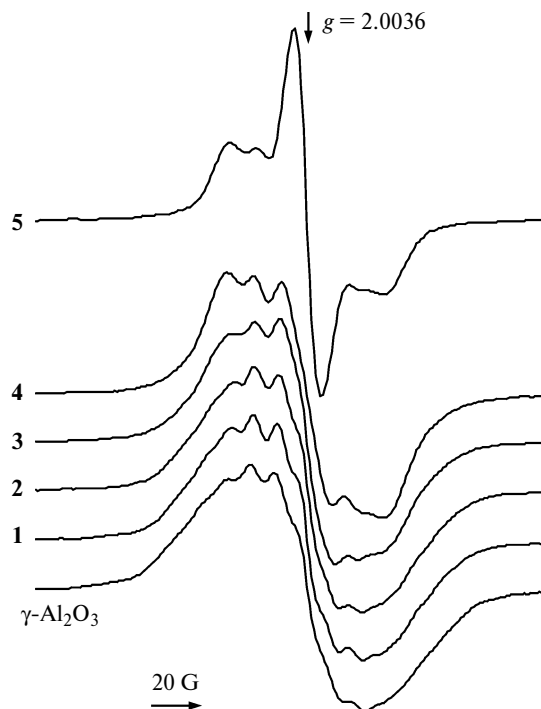


Fig. 1. ESR spectra of anthraquinone adsorbed on the surface of the $\gamma\text{-Al}_2\text{O}_3$ and $\text{Li}^+/\text{Al}_2\text{O}_3$ samples (1–5). The spectra were recorded at 20 °C.

Table 2. Concentration of the paramagnetic anthraquinone complexes on the surface of the alumina samples modified with lithium cations and the concentration of coordinatively unsaturated aluminum cations

Sample	Content of Li ⁺ /mmol (g of Al ₂ O ₃) ⁻¹	<i>N</i> · 10 ⁻¹⁶ /molecule m ⁻²			<i>N</i> _{LAS} · 10 ⁻¹⁶ /site m ⁻²
		Complex with two Al ³⁺ cations	Complex with one Al ³⁺ cation	Single line (in center)	
γ-Al ₂ O ₃	—	22	—	—	44
1	0.4	21	—	—	42
2	0.8	20.5	—	—	41
3	1.6	19	3.3	Traces	40
4	2.4	4.2	12	Traces	20
5	4	—	6.3	0.7	6.3

with one LAS.¹⁵ The changes in the concentration of the paramagnetic complexes and the concentrations of the coordinatively unsaturated Al³⁺ ions calculated as the sum of the doubled concentration of the complex with two Al³⁺ cations (eleven-component spectrum) and the concentration of the complex with one Al³⁺ cation (six-component spectrum) for the samples with different lithium contents are presented in Table 2. The concentration of the complex with one Al³⁺ cation passes through a maximum (see Table 2). For a higher lithium content (4 mmol of Li⁺ (g of Al₂O₃)⁻¹), a new spectrum appears as a single line in the center (*g* = 2.0036, ΔH_{pp} = 8.0 ± 0.2 G). The spectrum of the sample with the maximum lithium content is similar to those obtained earlier for the anthraquinone complex on the surface of the Li⁺/Al₂O₃ sample with the content 3.1 mmol of Li⁺ (g of Al₂O₃)⁻¹ (see Ref. 15) and LiAl₅O₈.¹⁶

Catalytic decomposition of isopropyl alcohol. The data on the change in the catalytic activity of Li⁺/Al₂O₃ obtained in a microcatalytic reactor are presented in Fig. 2. The catalytic activity of the Li⁺/Al₂O₃ samples passes through a maximum with an increase in the lithium content (see Fig. 2, curve 1), while it has previously⁵ been shown that the activity in isopropyl alcohol decomposi-

tion decreases as Li concentration decreases from 0.065 to 0.72 mmol g⁻¹.

Thermostimulated emission. The TSE data for the starting γ-Al₂O₃ and lithium-modified samples are shown in Fig. 3. Curve 1 corresponds to TSE upon the first heating of the starting samples, and curves 2 (see Fig. 3, *a–c*) and 3 (see Fig. 3, *d*) correspond to the TSE upon the repeated heating after desorption of adsorbed gases and vapors. Curves 3 (see Fig. 3, *a–c*) and 4 (see Fig. 3, *d*) were obtained after isopropyl alcohol was pre-adsorbed. It is seen that isopropyl alcohol adsorption on the samples heated to 360 °C results in a strong maximum of negative charge emission in the temperature interval from 100 to 200 °C. The maximum has a resolved structure and contains several peaks (breaks) characterizing, most likely, heterogeneity of the active surface. The large width of the maximum (at its half-height) indicates that the activation energies of charge emission are close in this temperature range. However, when larger amounts of lithium are introduced, the TSE decreases substantially both in terms of intensity and maximum width (see Fig. 3, *a*). The TSE curves of the starting samples mainly containing the *H₂O⁻, *OH⁻, *O₂⁻, and *CO₂⁻ ions are similar in shape to the TSE curves observed after isopropyl alcohol adsorption (see curves 1 and 3 in Fig. 3, *b*; curves 2 and 4 in Fig. 3, *d*). Protons and carbonium ions are not detected at a positive potential of the EE detector. This implies, probably, that the same sites are responsible for the emission of charges in the 100–200 °C interval from the starting samples and samples containing isopropyl alcohol. The sum of emitted charges determined from the surface area under the TSE curves (see Fig. 3, *a–d*) changes in parallel with the catalytic activity measured in the microcatalytic reactor (see Fig. 2).

The LAS concentration on the surface of the samples with a low lithium content (0.4–1.6 mmol g⁻¹) as determined from the highest concentration of the anthraquinone paramagnetic complex (see Table 2), remains virtually unchanged within the experimental error. However, the IR spectroscopic data for adsorbed carbon monoxide¹⁴ indicate that modification with lithium de-

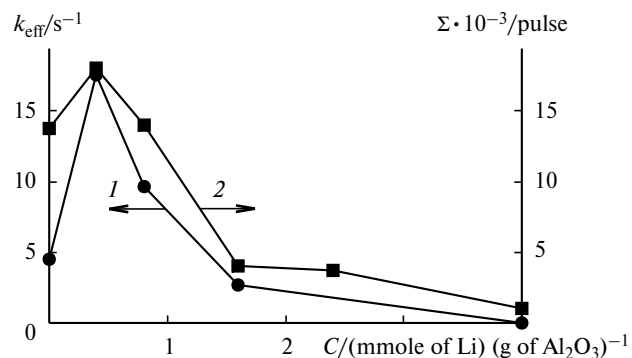


Fig. 2. Influence of the Li⁺ content on the catalytic activity (*k*_{eff}) of the Li⁺/Al₂O₃ samples at 260 °C (1) and the sum of thermostimulated emission charges emitted at 20–250 °C during isopropyl alcohol decomposition Σ (2).

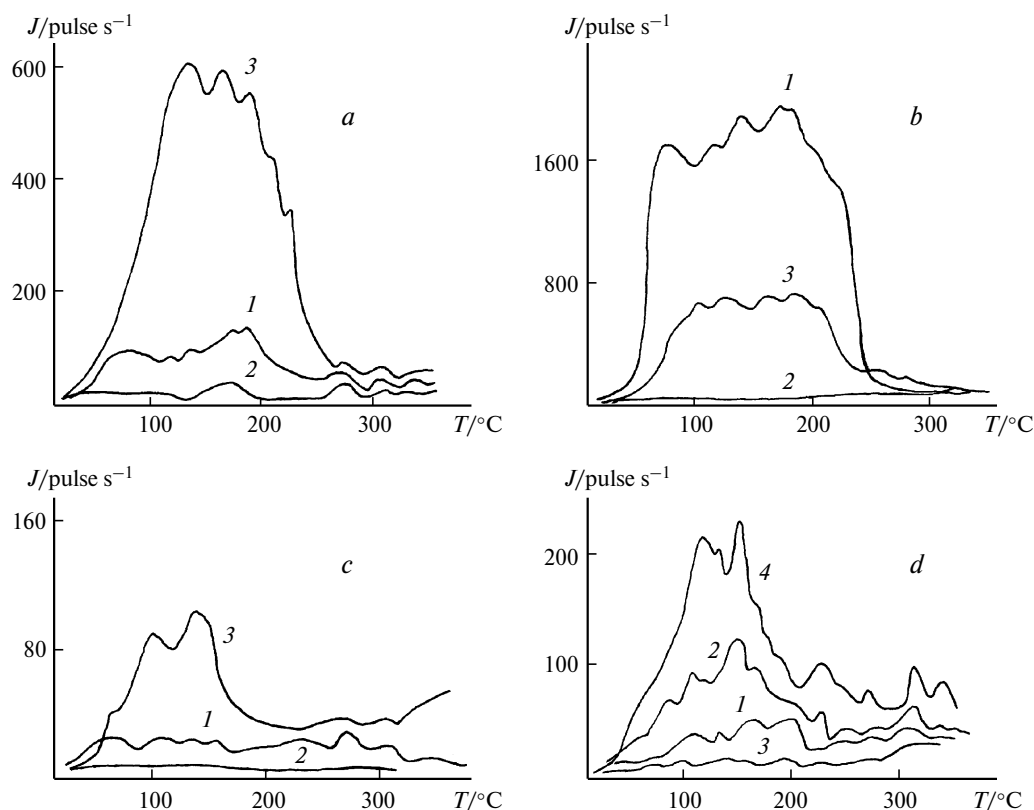


Fig. 3. *a–c.* Thermostimulated emission upon the first (1) and second (2) heatings of the starting $\gamma\text{-Al}_2\text{O}_3$ sample (*a*), sample 1 (*b*), and sample 3 (*c*) and after isopropyl alcohol adsorption (3). *d.* Thermostimulated emission upon the first (1), second (2), and third (3) heatings of sample 5 and after isopropyl alcohol adsorption (4).

creases both the amount of LAS and their strength. The apparent contradiction can be explained as follows. Anthraquinone is a hard base and can form complexes with LAS of different strength but similar in structure, whereas CO is quantitatively bound only by the strongest sites. Coverage of weak sites is low at conventional CO pressures of 20–30 Torr, and this leads to an underestimation of the total intensity of absorption bands. An earlier study on the adsorption of ammonia,¹⁷ also a stronger base than CO, revealed that the catalytic activity in isopropyl alcohol decomposition decreased with an increase in the lithium content, despite persistency or even some increase observed in the total acidity of LAS on the Li– Al_2O_3 surface. Since the radius of the Li^+ cations is small (0.068 nm),⁹ they can enter with some probability the alumina pore volume and, therefore, can hardly block LAS of the surface. However, the strength of the LAS can decrease due to the induction effect of lithium. Taking into account the mechanism of formation of the paramagnetic anthraquinone complex,¹⁵ the appearance of the six-component ESR spectrum is explained, most likely, by a considerable enhancement of the basicity of the $\text{Li}^+/\text{Al}_2\text{O}_3$ catalysts. In this case, it can be assumed that the interaction of anthraquinone with the LAS affords only a complex with one coordinatively unsaturated

Al^{3+} cation, because the strength of electron-acceptor sites is not strong enough for this complex to react with an additional Al^{3+} cation. The decrease in the strength of the LAS is also responsible, most likely, for the appearance of a single line, which should be attributed to anthra-semiquinone unbound or weakly bound with the LAS.¹⁸ The sample containing 4 mmol of Li^+ (g of Al_2O_3)^{−1} is similar by stoichiometry and structure to the LiAl_5O_8 aluminate.¹⁴ Although this aluminate resembles $\gamma\text{-Al}_2\text{O}_3$ in structure,¹⁹ its acidity is lower than that of alumina.

The influence of lithium on the catalytic activity of $\text{Li}^+/\text{Al}_2\text{O}_3$ is shown in Fig. 2. The data presented differ from the known results obtained in a flow reactor.^{5,6,17} According to these results, the Li^+ ions poison the activity of Al_2O_3 with respect to isopropyl alcohol, although we found an increase in the catalyst activity at a moderate lithium content. In several works,^{5,17} the authors observed a decrease in the catalytic activity in the dehydration reaction with an increase in the lithium content, although, according to the data of ammonia adsorption, the total acidity even increased weakly in this case. The decrease in the activity in dehydration upon the introduction of lithium into alumina can be due¹⁷ to a decrease in the concentration of the surface LAS. The difference in the data on the catalytic activity is related, most likely, to the

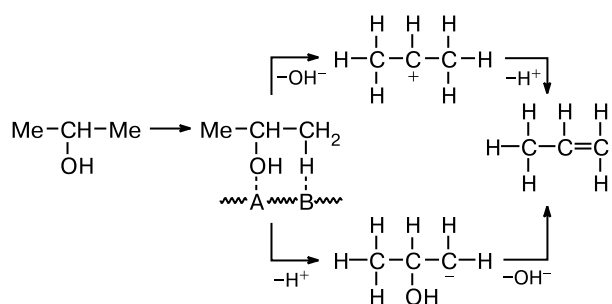
fact that some experiments^{5,17} were carried out in a flow-type reactor, whereas in the present work we used a pulse microcatalytic reactor. It is known^{20,21} for the pulse method that the reactions proceed in the nonstationary regime in the absence of poisoning of acid sites by reaction products. Therefore, the data yielded by the pulse method supplement the results obtained in flow-type systems.

An increase in the catalytic activity of Al_2O_3 upon the addition of small lithium amounts is confirmed by the data on EE accompanying the reaction in the adsorption layer. When the lithium content increases, both the activity in a pulse reactor and the sum of emitted negative charges of TSE pass through a maximum, and the catalysts lose their activity at a high lithium content. The dependence of the concentration of the paramagnetic anthraquinone complex with one Al^{3+} cation on the lithium content also passes through a maximum (see Table 2), although the position of this maximum does not coincide with the maximum in the activity curve. All these dependences agree with the assumption that as the lithium content increases acid sites are regularly weakened, while the basic sites are strengthened.

The dehydration of isopropyl alcohol affords water, propylene, and diisopropyl ether.⁵ In this case, water in the form of H_2O^- and OH^- can be removed from the same active sites that are present in the starting samples, which explains the TSE curves similar in shape (see Fig. 3) recorded upon isopropyl alcohol decomposition in the adsorption layer.

The catalytic dehydration of secondary alcohols on the acid-base sites of the metal oxide surface proceed according to Scheme 1 (see Ref. 22). This means that both the acid and basic sites affect the catalytic activity.

Scheme 1

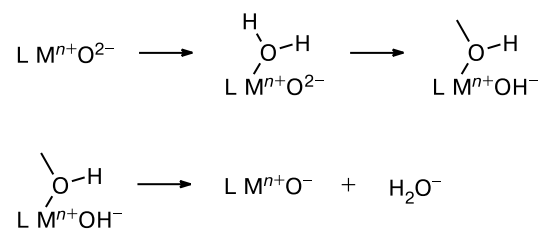


A is Lewis acid, B is Lewis base

In the system under study, coordinatively unsaturated metal cations can act as acid sites, and coordinatively unsaturated oxygen atoms are basic sites. At the same time, on the lattice fragments containing both acid and basic sites dissociative water adsorption occurs with the

tightening OH groups by acid sites followed by a possible emission of hydroxyls to the field of the positive EE detector²⁰ (Scheme 2).

Scheme 2



L is oxide lattice

Based on the proposed mechanism, we can conclude that the dehydration of secondary alcohols affords cations (H^+ , carbonium ions), which are not detected at a positive potential of the EE detector, and also negative ions (OH^- and carbanions) recorded by the EE detector during isopropyl alcohol decomposition in the adsorption layer (see Figs 2–5) occurring at 20–250 °C. Exo-emission increases at low lithium additives predominantly due to an increase in the basicity of sites upon the formation of the $[\text{Al}-\text{OH}]-\text{Li}^+$ groups but then decreases due to the competitive process of LAS poisoning with lithium. The catalytic activity changes similarly: at low lithium concentrations the increase in the basic properties is more pronounced than some decrease in acidity. Therefore, the catalyst activity increases. Both the strength and concentration of LAS decreases at a high lithium content. As a result, the rate of isopropyl alcohol decomposition decreases, because this reaction occurs only when the acid and basic sites, whose strength and concentration are rather high, are present on the catalyst surface.

Thus, the results obtained in a microcatalytic reactor, unlike published data for a flow-type reactor, indicate that small lithium additives activate the $\text{Li}^+/\text{Al}_2\text{O}_3$ catalysts in the decomposition of isopropyl alcohol. This conclusion was also made in the study of the EE of negative charges that characterize electron-acceptor surface sites *in situ* during the reaction in the adsorption layer. According to the ESR data using anthraquinone as a probe molecule, the total amount of LAS remains unchanged upon introduction of 0.04 to 1.6 mmoles of Li^+ (g of Al_2O_3)⁻¹. The mechanism for the decomposition of isopropyl alcohol on the $\text{Li}^+/\text{Al}_2\text{O}_3$ catalysts involving both electron-donor and electron-acceptor sites was proposed. It was shown that the modification of alumina with Li^+ cations introduced in small amounts (to 1.7 wt.%) did not result in selective poisoning of acid sites of the surface.

The authors are grateful to G. P. Murav'eva for performing powder X-ray diffraction analysis and E. P. Chinennikova for measuring the specific surface of the samples.

This work was financially supported by the Federal Agency on Science and Innovations (State Contract 02.451.11.7012 of August 29, 2005), the Council on Grants of the President of the Russian Federation (Program of State Support for Leading Scientific Schools of the Russian Federation, Grant RI-112/001/056), the Scientific Program "Universities of Russia" (Grant UR.05.02.549), and the Russian Foundation for Basic Research (Project No. 06-03-32830a).

References

1. Y. Fu, T. Baba, and Y. Ono, *Appl. Catal.*, 1998, **166**, 419.
2. Y. Fu, T. Baba, and Y. Ono, *Appl. Catal.*, 1998, **166**, 425.
3. S. Narayanan and K. Uma, *J. Chem. Soc., Faraday Trans. 1*, 1987, **83**, 733.
4. N.-A. M. Deraz, H. H. Salim, and A. Abd El-Aal, *Mater. Lett.*, 2002, **53**, 102.
5. G. G. Cortez, S. R. de Miguel, O. A. Scelza, and A. A. Castro, *J. Chem. Tech. Biotechnol.*, 1992, **53**, 177.
6. A. Gervasini, J. Fenyvesi, and A. Auroux, *Langmuir*, 1996, **12**, 5356.
7. E. V. Lunina, M. N. Zacharova, G. L. Markaryan, and A. V. Fionov, *Coll. Surf. A: Physicochem. Eng. Asp.*, 1996, **115**, 195.
8. I. V. Krylova, *Khimicheskaya elektronika (elektronnye i ionnye yavleniya, soprovozhdayushchie fiziko-khimicheskie prevrashcheniya na poverkhnosti tverdykh tel)* [Chemical Electronics (Electronic and Ionic Phenomena Accompanying Physicochemical Transformations on the Solid Surface)], Izd-vo Mos. Gos. Univ., Moscow, 1993, 167 pp. (in Russian).
9. *Spravochnik khimika*, Ed. B. P. Nikol'skii, Gos. Nauchno-Tekhn. Izd-vo Khimicheskoi Literatury, Leningrad—Moscow, 1963, **1**, 475 (in Russian).
10. A.s. 1012115A SSSR; *Byul. Izobret.* [Author's Certificate 1012115A USSR; *Invention Bulletin*], 1983, No. 14 (in Russian).
11. A. V. Fionov, Ph. D. (Chem.) Thesis, M. V. Lomonosov Moscow State University, Moscow, 1994, 172 pp. (in Russian).
12. I. V. Krylova, N. A. Oks, and V. I. Svitov, *Zav. Labor.*, 1982, **48**, 55 [*Ind. Lab.*, 1982, **48** (Engl. Transl.)].
13. I. V. Krylova, N. I. Konyushkina, I. A. Rodina, and V. I. Svitov, *J. Catal.*, 1979, **60**, 8.
14. S. R. de Miguel, O. A. Scelza, A. A. Castro, and J. Soria, *Topics Catal.*, 1994, **1**, 87.
15. A. V. Fionov, *Surf. Sci.*, 2002, **507**—**510**, 74.
16. A. V. Fionov, A. Ospan, E. V. Lunina, V. P. Isupov, R. P. Mitrofanova, and L. E. Chupakhina, *Tez. dokl. X Mezhdunar. konf. "Magnitnyi rezonans v khimii i biologii" [Abstrs X Intern. Conf. "Magnetic Resonance in Chemistry and Biology"] (Suzdal', June 1—7, 1998)*, Suzdal', 1998, 62 (in Russian).
17. A. Gervasini, J. Fenyvesi, and A. Auroux, *Catal. Lett.*, 1997, 219.
18. A. V. Fionov, I. M. Zaitseva, A. N. Kharlanov, and E. V. Lunina, *Kinet. Katal.*, 1997, **38**, 155 [*Kinet. Catal.*, 1997, **38**, 139 (Engl. Transl.)].
19. P. Tarte, *Spectrochim. Acta*, 1967, **23A**, 2127.
20. H. Bremer and K.-P. Wendlandt, *Heterogene Katalyse*, Akademie Verlag, Berlin, 1978, 211.
21. A. L. Rozental', in *Problemy kinetiki i kataliza. XV. Mekhanizm i kinetika geterogennykh reaktsii* [Problems of Kinetics and Catalysis. XV. Mechanism and Kinetics of Heterogeneous Reactions], Nauka, Moscow, 1973, p. 163 (in Russian).
22. K. Tanabe, *New Solid Acids and Bases: Their Catalytic Properties*, Kodansha, Tokyo, 1989, 365 pp.

Received April 5, 2005;
in revised form December 28, 2005